Journal of the European Ceramic Society **8** (1991) 243–250

Growth of Aluminium Nitride Crystal Under a Nitrogen Transferred Arc Plasma

H. Ageorges, Chang Kun, S. Megy, E. Meillot, A. Sanon & J. M. Baronnet

Laboratoire de Chimie des Plasmas, Université de Limoges, 123 avenue A. Thomas, 87060 Limoges Cédex, France

(Received 18 December 1990; revised version received 11 March 1991; accepted 15 March 1991)

Abstract

Ultrafine particles of aluminium nitride (AlN) are produced by a transferred arc plasma on aluminium metal in nitrogen or nitrogen/hydrogen atmospheres. They are collected in a bag filter and on the walls of the reaction chamber. The powder is confirmed to be hexagonal AlN with a few metal aluminium traces.

A growth of an aluminium nitride crystal from molten Al under the arc is observed. It is sectioned vertically in halves and examined by light and electron microscopy, and analysed by XRD and electron probe microanalysis. It consists of about equal amounts of Al metal and AlN with an increase in AlN towards the top. This mode of occurrence of the AlN crystallites in the Al matrix shows that it is a good composite. Five different textures, observed in this crystal, suggest a complex history of crystallization.

Extrem feine AlN-Körner wurden dadurch hergestellt, daß Aluminium in einer Stickstoff- bzw. Stickstoff/Wasserstoff-Atmosphäre einem Plasma ausgesetzt wurde. Die Teilchen wurden in einem Staubfilter und von den Wänden des Rezipienten gesammelt. Das Pulver besteht aus hexagonalem AlN mit geringen Spuren metallischen Aluminiums. Unter dem Plasmabogen bildet sich aus geschmolzenem Aluminium ein AlN-Kristall. Er wurde in vertikaler Richtung halbiert und mittels Lichtmikroskop, Elektronenmikroskop, Röntgenbeugung und Mikrosonde untersucht. Er besteht aus etwa gleichen Anteilen Aluminium und AlN, wobei der AlN-Anteil zur Spitze hin zunimmt. Diese Ko-Existenz der AlN-Kristalle in der Aluminiummatrix weist auf einen guten Verbundwerkstoff hin. Fünf unterschiedliche Texturen, die in diesem Kristall zu beobachten sind, sind ein Indiz für ein komplexes Kristallisationsverhalten.

Des particules ultrafines de nitrure d'aluminium (AlN) sont produites par un plasma d'arc transféré sur un bain d'aluminium sous atmosphère d'azote ou d'azote/hydrogène. Elles sont collectées dans un filtre à manche et sur les parois du réacteur. La poudre s'avère être de l'AlN quelques traces d'aluminium métal.

La croissance d'un cristal sur le bain d'aluminium sous le pied d'arc est observée. Les résultats des analyses par diffraction X et microsonde en microscopies optique et électronique des différentes textures du cristal sont présentés. Il est constitué d'Al métal et de AlN en quantité égale avec, cependant, une augmentation du taux de AlN vers le sommet. Ce mode d'insertion de cristallites de AlN dans la matrice Al indique que c'est un composite remarquable. Cinq textures différentes, observées dans ce cristal, suggèrent une histoire de cristallisation complexe.

1 Introduction

Aluminium nitride has satisfactory properties as a ceramic material.[1] AlN provides a range of thermal conductivity for increased flexibility in solving thermal management problems. Its thermal conductivity (up to 220 W/(mK)) can approach that of beryllia, which is penalized by its toxicity. AlN has a high electrical resistivity ($>10^{14}\,\Omega$ cm) similar to alumina, making it a good insulator for electronic or other applications requiring electrical insulation. The very low thermal coefficient of expansion, similar to silicon, provides a high thermal shock resistance.

A sintered substrate has these properties when:

—The initial powders have a high purity; the presence of oxygen impurities causes practical problems. The effect of oxygen content in

Journal of the European Ceramic Society 0955-2219/91/$3.50

sintered AlN on its thermal conductivity was examined by Kuramoto *et al.*;[2] it was found that the thermal conductivity is drastically affected and drops from 145 to 80 W/(mK) when the oxygen rate increased from 0·1 to 2%.

—The average size of the particles is less than 0·5 μm.

—These particles are dispersed.

Also its price must be competitive regarding industrial production.

AlN synthesis through carbothermal reduction, either of Al_2O_3[3-12] or aluminium hydroxide,[13,14] or produced by the direct nitridation of aluminium metal with either nitrogen or ammonia,[15-17] provides both metallic and oxygen impurities. Aluminium nitride prepared in this way has low specific surface (less than 0·5 m^2/g).[18] So the items made from it need a high temperature (2000 K) for sintering and have considerable porosity (more than 5%).

That is why many studies have been undertaken to synthesize ultrafine powders by the vapour-phase reaction of nitrogen or ammonia on aluminium chloride,[19-23] or triisobutylaluminium,[24] for example.

Another method to produce ultrafine powders is the plasma process:

—A radio frequency induction plasma[25] is used to synthesize ultrafine nitride powder from aluminium metal.

—The arc plasma reactor[18,26-35] uses as raw material powders or ingots of aluminium; the process is common,[27] the production rates are important and the price should become competitive.

The process described in this paper is especially easy: a nitrogen arc is transferred on an aluminium ingot. By the thermal energy of the plasma the metal is melted and metal atoms are vaporized from the metal surface, and the nitrogen or ammonia as plasma-forming gas gives N atoms, N_+ ions, electrons and small amounts of N_2. The aluminium melt is supersaturated in nitrogen atoms which escape out of the arc and react in the vapour phase with Al vapour to produce aluminium nitride.

After a thermodynamic approach of the process and a brief description of the experimental set-up, the AlN formation and the results are discussed.

2 Equilibrium Modelling of the Synthesis

The assumptions of complete thermodynamic equilibrium are probably not confirmed in the low temperature areas, in particular at the solid–gas interface. But the equilibrium prediction can forecast the possible compounds, the chemical composition in the final product and suggest the best quenching temperature.

A computer program of the chemical composition is based on the minimization of Gibbs free energy G of the system by steepest descent with, as objective function, the Lagrange function obtained from the Taylor development of G/RT and from the mass balance constraints, according to White *et al.*[36]

In order to calculate the total free energy of the system, values of the basic thermodynamic quantity used, namely G/RT, have to be specified for all species considered. Therefore, if a species appears in two or more phases, values which are specific for each phase must be used.

Tabulated values of thermodynamical quantities for species in the solid, liquid and gaseous state are to be found in the JANAF Thermodynamical Tables.[37] Lagrange's method of undetermined multipliers is

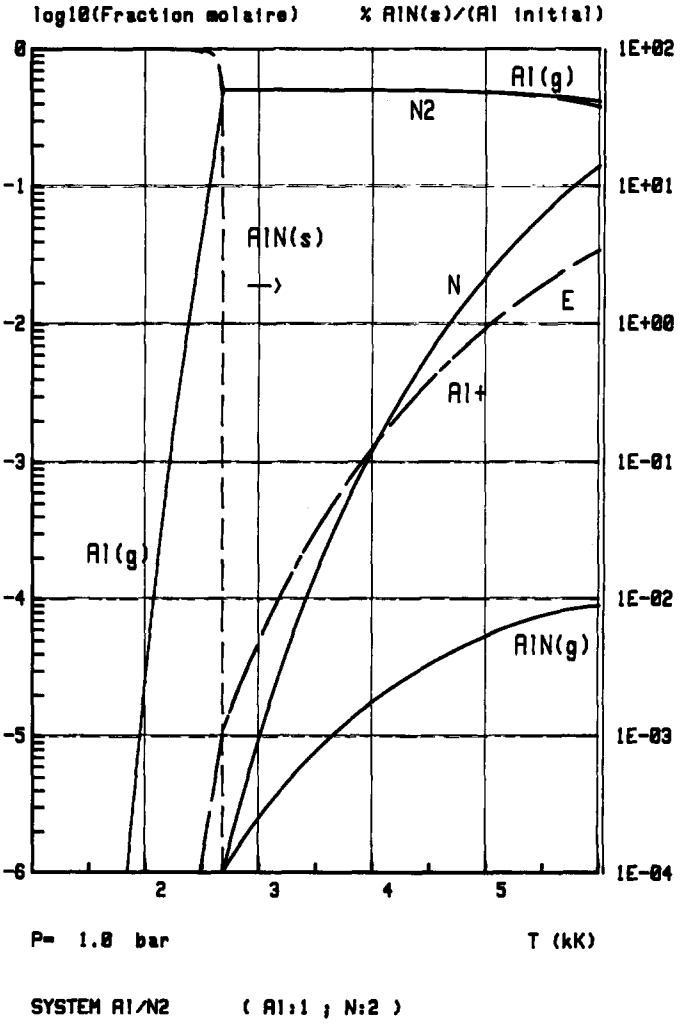

Fig. 1. Chemical composition of the Al/N_2 system (Al = 1; N = 2).

used for determining the constrained minimum with the mass balance constraints. The derivative equations thus obtained are expanded in a Taylor series about initially estimated n_i-values, neglecting terms involving derivatives of second and higher orders.

The equilibrium amounts are therefore obtained after a series of iterations. From the first approximate solution improved n_i-values are calculated and used as new initial estimates in the subsequent iteration cycle. This procedure is repeated until constant n_i-values are achieved, provided that the set of phases chosen are found to be the equilibrium phases.

In Fig. 1 is plotted the chemical composition of an Al/N_2 system (2 atoms nitrogen to 1 atom aluminium). This diagram shows on the one hand the molar fractions of each species in the vapour phase and on the other hand, on the right-hand scale, the rate of conversion of Al into AlN solid in comparison with initial aluminium versus temperature. Solid aluminium nitride formed with 1 mol aluminium and 1 mol nitrogen is stable up to 2500 K. Then, above this temperature, AlN(s) starts slowly decomposing until 2680 K, where it disappears completely. AlN(s) is transformed into aluminium vapour, which can recombine with nitrogen to form AlN(s). As noted earlier, there is no liquid phase of AlN. In this composition neither solid nor liquid aluminium is available for the Al/N reaction rate; AlN is the only solid-phase product below 2700 K, so its complete conversion is possible. Between 2700 and 5500 K aluminium and molecular nitrogen are equimolar. Nitrogen dissociation is significant above 5000 K.

3 Experiment

Figure 2 shows the schematic view of the transferred arc plasma reactor. The chamber consists of a double wall made of stainless steel with a water-cooled system. Its inside diameter is 40 cm. To increase the vaporization of aluminium the temperature must be as high as possible (between 2000 and 2500°C). Instead of refractory lining, a layer of rigid graphite wool and a system of two graphite furnaces were put inside the steel vessel for thermal insulation and to increase temperature at the same time.

The arc is struck between a movable thoriated tungsten cathode and a movable anode. The anode, made of a pure aluminium (99·9%) ingot, is inserted into a graphite crucible which is surrounded by a water-cooled stainless-steel support. Nitrogen or a mixture of nitrogen and hydrogen is introduced around the cathode. In some experiments ammonia is used as a jacket plasma gas.

Typical operating conditions were as follows:

Current	200 A	→ Power 18 kW
Voltage	90 V	
Nitrogen flow rate	21 normal litre/min (N litre/min)	
Hydrogen flow rate	15 N litre/min	
Electrode gap	~110 mm	

The exhaust gases are evacuated through the quenching module, where nearly 100 N litre/min of nitrogen or ammonia is introduced. Then they run through a cooled cyclone system, a heat exchanger and the powders are collected in a bag filter made of dralon.

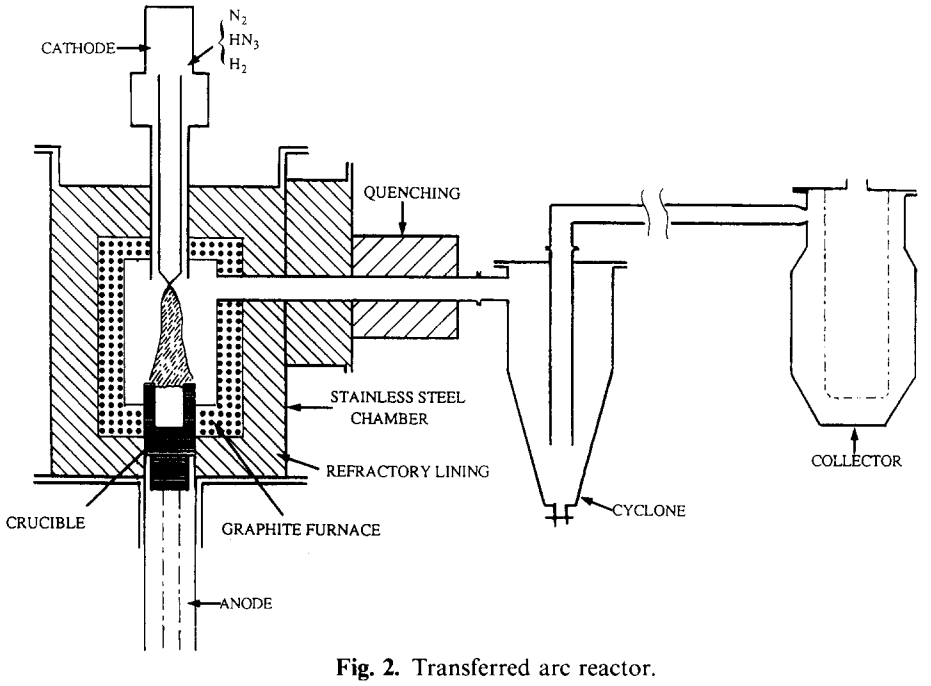

Fig. 2. Transferred arc reactor.

4 Results and Discussion

4.1 Experimental procedure

As soon as the arc is struck under nitrogen the instantaneous growth of crystals and dendrites is observed on the initially flat surface of the aluminium ingot. Then, whereas the growth of the crystal and dendrite decreases, in the centre, on the aluminium block, a large crystal forms very quickly at about 2 to 5 mm/min. The growing velocity decreases while the crystal increases. The growth stops when the height is about 5 cm.

In the first minutes, and during ultrafine powder formation, a fog is observed in the reaction chamber, showing a high production rate of ultrafine powders. Moreover, liquid aluminium droplets are observed sweating through the porosities of the 'crystal' at the upper part, where the arc foot walks on the complicated surface.

4.2 Crystal analysis

Under the 'crystal' an important cavity is observed (Fig. 3) with smooth walls, probably where liquid aluminium was during the experimentation. This rose by capillarity in the complex structure and diffused through the porous wall.

The 'crystal' has been examined and analysed with the help of Billiton Research (The Netherlands). It was sectioned vertically in halves; one half was examined by light and electron microscopy, and analysed by XRD and electron probe microanalysis.

XRD showed the presence of aluminium metal and AlN in similar proportions with an increase in AlN towards the top. By light microscopy five different textures were identified; the distribution of the textures over the cross-section of the 'crystal' is shown in Fig. 4.

Texture A, in the core of the large 'crystal', is a very porous microstructure with a eutectic texture. The

Fig. 3. 'Crystal' formed under nitrogen atmosphere.

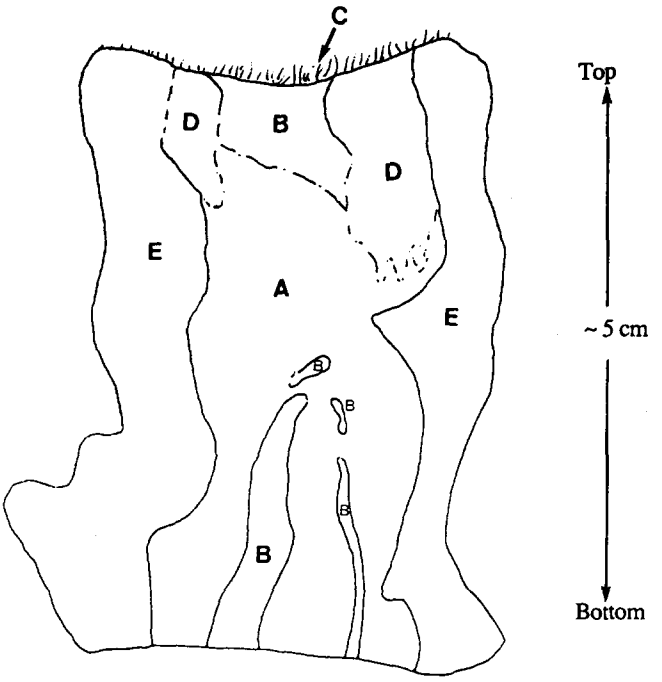

Fig. 4. Schematic distribution of textures in cross-section of 'crystal' sample. A, Very porous microstructure with eutectic texture; B, dense banded mixture; C, dendrites; D, massive coarse-grained AlN; E, dense microstructure with homogeneously dispersed AlN crystallites.

proportion of Al and AlN is estimated at 50/50 overall. The porosity is estimated at 30% (Fig. 5). The size of the AlN crystallites varies considerably: fine lamellas and blebs in the intergrowth are 5–10 μm in size/thickness, but coarser particles are 100–200 μm (Figs 6 to 10). Some parts of this texture show resorbed hexagonal crystals: the hexagonal rim is still observed but the core of the crystals consists of aluminium metal (Fig. 10).

Texture B, in the axis of the 'crystal' at the bottom (Fig. 11) and at the top (Fig. 12), shows a dense banded texture. Rounded to hexagonal crystallites

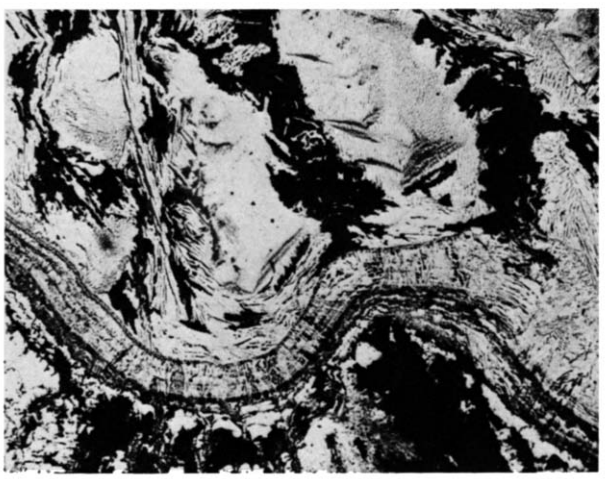

Fig. 5. Crystal texture A (with thin band of texture B): light micrography of a polished surface; porosity is black, aluminium metal is white.

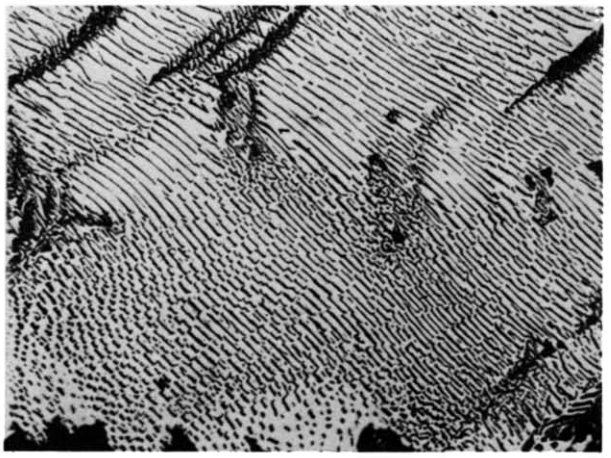

Fig. 6. Crystal texture A: close-up of Fig. 5; AlN is grey, Al is white.

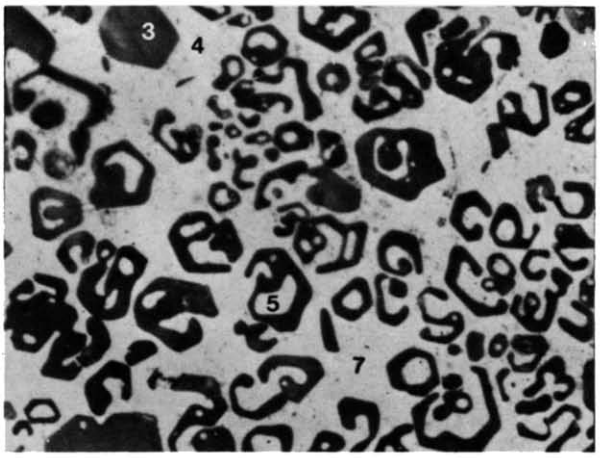

Fig. 9. Crystal texture A: close-up of Fig. 7 showing resorbed AlN crystals (grey) in Al matrix (white).

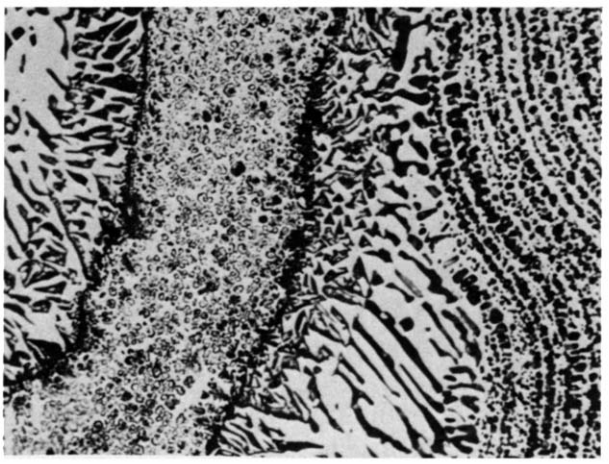

Fig. 7. Crystal texture A: light micrography of polished surface showing 'normal' AlN crystals with an hexagonal closed structure (Fig. 8) and resorbed AlN crystals with an hexagonal open structure (Fig. 9); AlN is grey, Al matrix is white.

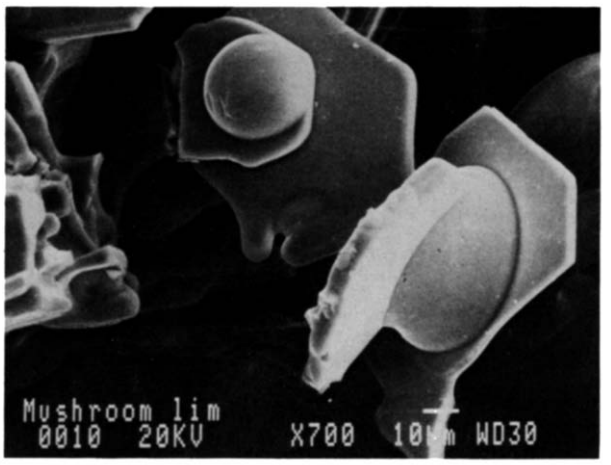

Fig. 10. Crystal texture A showing AlN platelets and droplets of Al metal in the core.

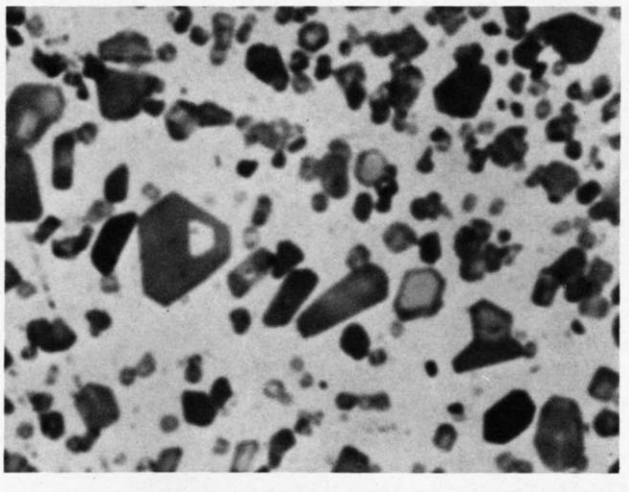

Fig. 8. Crystal texture A: close-up of Fig. 7 showing 'normal' AlN crystals (grey) in Al matrix (white).

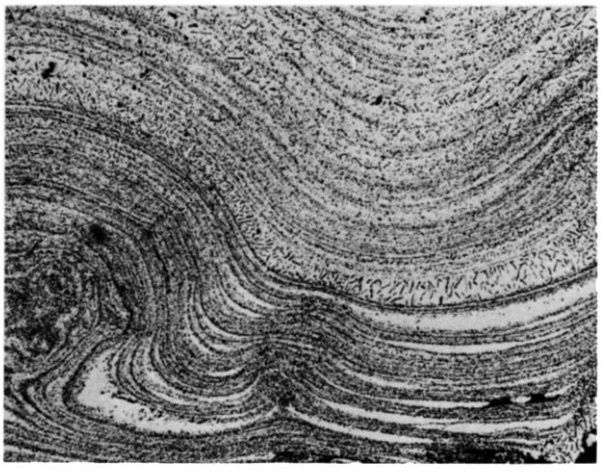

Fig. 11. Crystal texture B, in lower centre; light micrography of polished surface: individual layers made up of fine AlN crystallites (grey).

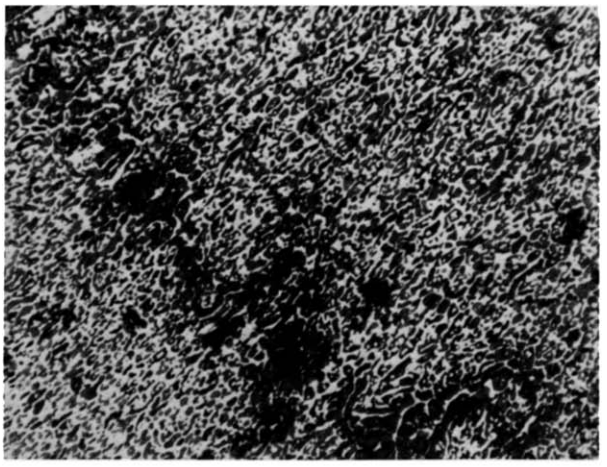

Fig. 12. Crystal texture B, near the top; light micrography of polished surface: AlN crystallites.

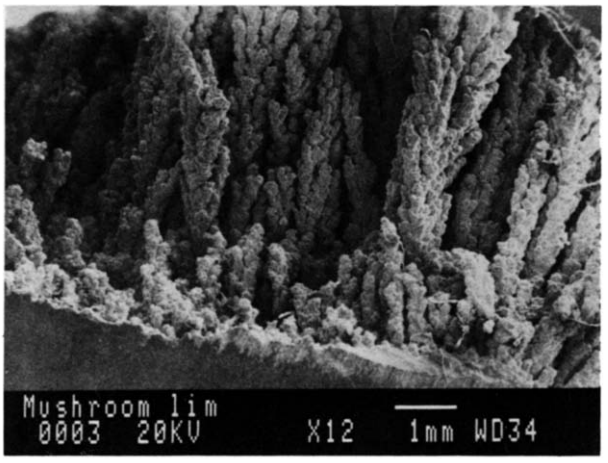

Fig. 13. Texture C at the top of the 'crystal' dendrite observed by scanning electronic microscopy.

Fig. 14. Texture C at the top of the 'crystal': close-up of dendrite in Fig. 13.

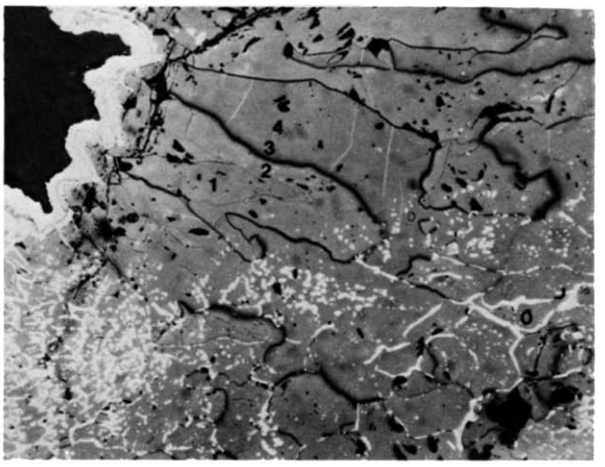

Fig. 15. Texture D near the top of the 'crystal'; light micrography: massive AlN (Al is white).

of 20–50 μm occur, largely homogeneously dispersed, but densely accumulated AlN crystals from thin bands/lamellas. These bands are mostly curved. The proportion of Al to AlN is estimated at 50/50 in the top and 65/35 in the bottom of the 'crystal'.

Texture C is observed with dendrites only on the top of the 'crystal' (Fig. 4). AlN mostly forms the core of the dendrites and Al the shell (Figs 13 and 14).

Texture D occurs in the top of the 'crystal' outside of the axis. It is made of massive coarse-grained AlN. The AlN forms large elongated crystallites. The amount of Al metal associated with this texture is less than 10% (Fig. 15).

On each side of the 'crystal' texture E is observed. It is a dense microstructure with homogeneously dispersed AlN crystals of 1–15 μm (Fig. 16). The proportion of Al to AlN is estimated at 50/50. The outer boundary of the 'crystal' consists fully of AlN.

The mode of occurrence of the AlN crystallites in the Al matrix suggests that this texture is a very good

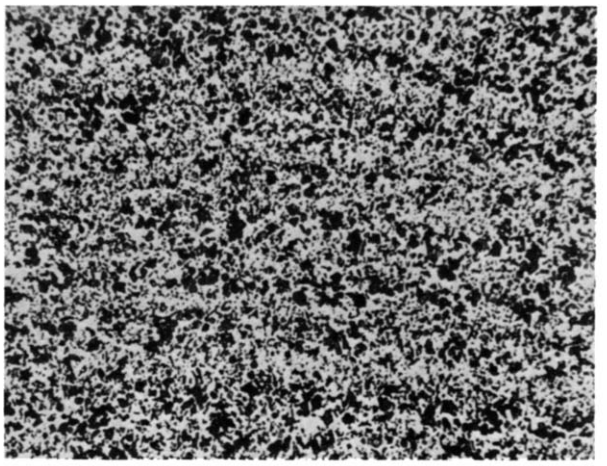

Fig. 16. Texture E in each side of the 'crystal'; light micrography of polished surface: homogeneously dispersed AlN crystallites (grey) in Al metal.

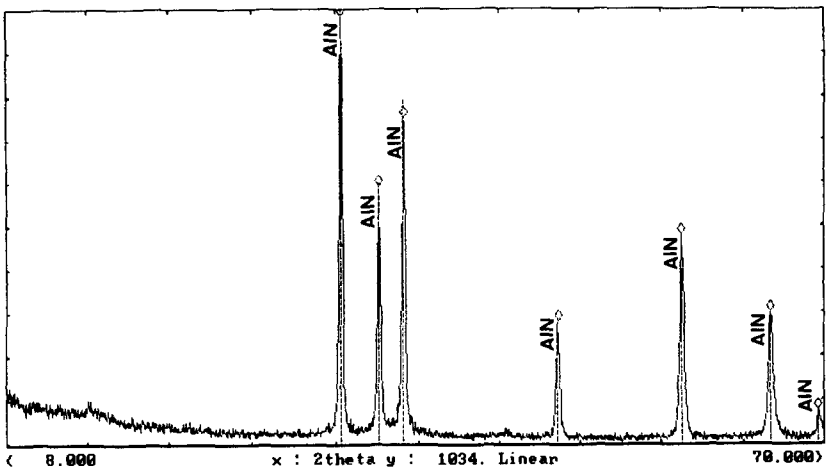

Fig. 17. X-Ray diffraction pattern of the powders collected on the walls of the reactor.

composite. The textures observed suggest a complex history of crystallization.

4.3 Powders analysis

The powders deposited on the reactor walls are white and in the bag filter grey. The X-ray diffraction spectrum (Fig. 17) shows the presence of only aluminium nitride. Figure 18 is a photograph of analysis by transmission electron microscopy of the powders collected in the bag filter. The fine material is composed of hexagonal submicron particles, which is typical of an AlN structure.

The powder size is between 10 and 100 nm. The BET-specific surface varies between 10 and 50 m^2/g.

Chemical analysis has shown some trace of unreacted aluminium metal in the powder collected in the bag filter, whereas the powder from the wall of the reactor is only aluminium nitride but with some whiskers. The authors suggest that the unreacted aluminium powders are due to an excess of aluminium in the vapour phase or an insufficient reaction time. Injecting only a small percentage of NH_3 into the plasma rapidly diminishes the aluminium content of the powder.

The high content of oxygen (3–6%) in the powder is apparently due to the oxidation of fine aluminium powder and the interaction of fine AlN powder with humidity in the air when the product powder is exposed to the air after each experiment.

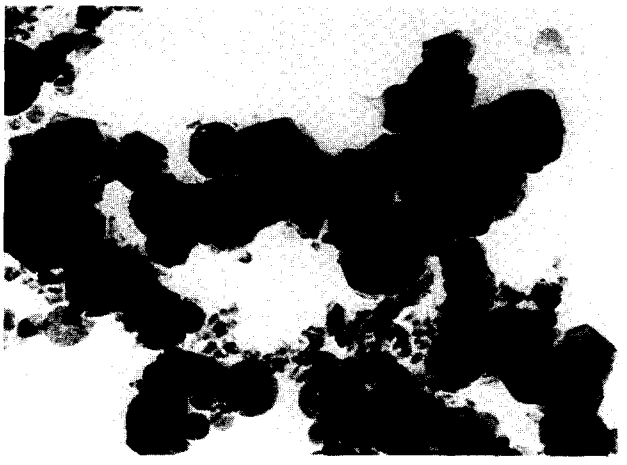

Fig. 18. Transmission electronic micrography of the powders collected in the bag filter: test in nitrogen/hydrogen atmosphere.

Acknowledgements

This research is supported by a BRITE contract with the collaboration of Tetronics Research and Development, UK; Billiton Research, The Netherlands; and GH Industrial, Spain.

The authors wish especially to acknowledge J. Williams and C. Forty (Tetronics R&D) for many helpful discussions and suggestions during this work, and D. Canham and his colleagues (Billiton Research) for their help in the 'crystal' analysis.

The authors thank J. Jarrige, J. P. Laval and P. Lortholary (University of Limoges) for their participation in the powders analysis.

References

1. Standard Oil (USA), Form A-14,054, Rev 11/87, 1987.
2. Kuramoto, N., Taniguchi, H. & Aso, I., *IEEE Transactions on Components Hybrids and Manufacturing Technology*, **CHMT-9**(4) (1986) 386.
3. Bachelard, R. & Joubert, P., *Materials Science and Engineering*, **A109** (1989) 247.
4. Silverman, L. D., *Advanced Ceramic Materials*, **3**(4) (1988) 418.
5. Hirai, S., Miwa, T., Iwata, T. & Katayama, H., *J. Japan Inst. Metals*, **54**(2) (1990) 181.
6. Bachelard, R. & Joubert, P., French Patent No. 2 596 745, 1986.
7. Inoue, H., Tsuge, A. & Komeya, K., European Patent No. 0 176 737-A1, 1986.

8. Inoue, H., Tsuge, A. & Komeya, K., US Patent No. 4 615 863, 1986.
9. Inoue, H., Tsuge, A. & Komeya, K., US Patent No. 4 680 278, 1987.
10. Li, W. I., Huang, L. P., Huang, X. Z., Kuang, G., Tan, S. H., Fwu, S. R. & Yen, T. S., In *Ceramics Powders*, ed. P. Vincenzini. Elsevier Scientific Publishing Co., Amsterdam, 1983, p. 403.
11. Lefort, P., Marty, F., Ado, G. & Billy, M., *Revue de Chimie Minérale*, **22** (1985) 534.
12. Rocherulle, J., Guyader, J., Verdier, P. & Laurent, Y., *Rev. Int. Hautes Tempér. Réfract.*, **22** (1985) 83.
13. Mitomo, M. & Yoshioka, Y., *Advanced Ceramic Materials*, **2**(3A) (1987) 253.
14. Sugahara, Y., Yokoyama, N., Kuroda, K. & Kato, C., *Ceramics International*, **14** (1988) 163.
15. Kimura, I., Ichiya, K., Ishii, M., Hotta, N. & Kitamura, T., *J. Mater. Sci. Letters*, **8** (1989) 303.
16. Belau, A. & Muller, G., *Cfl/Ber. DkG*, **65**(5) (1988) 122.
17. Hotta, N., Kimura, I., Tsukuno, A., Saito, N. & Matsuo, S., *Yogyo-Kyokai-Shi*, **95**(2) (1987) 274.
18. Vissokov, G. P. & Brakalov, L. B., *J. Mater. Sci.*, **18** (1983) 2011.
19. Riedel, R., Petzow, G. & Klingebiel, U., *J. Mater. Sci. Letters*, **9** (1990) 222.
20. Kimura, I., Hotta, N., Nukui, H., Saito, N. & Yasukawa, S., *J. Mater. Sci.*, **24** (1989) 4076.
21. Watari, T., Akizuki, T., Ikeda, H., Torikai, T. & Matsuda, O., *J. Ceram. Soc. Jpn Inter. Ed.*, **97** (1989) 851.
22. Lewis, D. W., *J. Electrochem. Soc.*, **117**(7) (1970) 978.
23. Kimura, I., Hotta, N., Nukui, H., Saito, N. & Yasukawa, S., *J. Mater. Sci. Letters*, **7** (1988) 66.
24. Tsuchida, K., Takeshita, Y., Yamane, A. & Kato, A., *Yogyo-Kyokai-Shi*, **95**(12) (1987) 1198.
25. Baba, K., Shohata, N. & Yonezawa, M., In *8th International Symposium on Plasma Chemistry*, Tokyo, 1987, p. 2034.
26. Uda, M., Ohno, S. & Okuyama, H., *J. Ceram. Soc. Jpn Inter. Ed.*, **95** (1987) 70.
27. Uda, M. & Ohno, S., *The Chemical Society of Japan*, **6** (1984) 862.
28. Shah, A. & Etemadi, K., In *8th International Symposium on Plasma Chemistry*, Tokyo, 1987, p. 2071.
29. Matsumoto, O., Shirato, Y. & Miyazaki, M., *J. Electrochem. Soc. Japan*, **36**(4) (1968) 219.
30. Matsumoto, O., *J. Electrochem. Soc. Japan*, **36**(4) (1968) 207.
31. Matsumoto, O., *Denki Kagaku*, **35** (1967) 697.
32. Matsumoto, O. & Shirato, Y., *Denki Kagaku*, **39** (1971) 82.
33. Ishizaki, K., Egashira, T., Tanaka, K. & Celis, P. B., *J. Mater. Sci.*, **24** (1989) 3553.
34. Bourdin, E., Thèse de 3ème cycle, Université de Limoges, 1976.
35. Pfender, E. & Lu, Z. P., In *9th International Symposium on Plasma Chemistry*, Italy, 1989, p. 675.
36. White, W. B., Johnson, S. M. & Dantzig, G. B., *J. Chem. Phys.*, **28**(5) (1958) 751.
37. JANAF, *Thermochemical Tables*, Third Edition, 1985. Published by the American Chemical Society and the American Institute of Physics for the National Bureau of Standards.